doi.org/10.36721/PJPS/2026.40.16875.1

Network pharmacology analysis of Xinbao Pill against heart failure with preserved ejection fraction

Jianmin Shao[1], Xiang Yu[1], Xiaobing Zhang[2], Shiqiang Chen[2] and Dawei Huang[2]*
[1]Yongjia Hospital of Traditional Chinese Medicine, Yongjia, Zhejiang, China
[2]The People's Hospital of Yuhuan, Yuhuan, Zhejiang, China

Abstract: **Background**: Heart failure with preserved ejection fraction (HFpEF) accounts for approximately half of all heart failure cases and lacks effective targeted therapy. Traditional Chinese medicine formulas, such as Xinbao Pill, have shown potential cardiovascular benefits; however, their molecular mechanisms are not yet fully understood. **Objectives**: This study aimed to systematically explore the multi-compound, multi-target mechanism of Xinbao Pill in the treatment of HFpEF using a network pharmacology approach. **Methods**: Active ingredients of Xinbao Pill were identified from the TCMSP database according to predefined pharmacokinetic criteria. Three GEO datasets (GSE180065, GSE240400 and GSE269053) were analyzed to identify differentially expressed genes associated with HFpEF. Elastic Net regression was used to refine the intersecting targets. Molecular docking and 100 ns all-atom molecular dynamics simulations were used to predict and validate the structural stability of compound-target interactions. **Results**: A total of 32 active compounds were identified. Differential expression analysis identified 1,368 HFpEF-related genes across the three datasets, including 23 overlapping targets. Elastic Net regression further selected 11 key genes (Clk1, Comt, Drd2, Ephx2, Fgr, Hcn2, Mme, Pparg, Ptgds, Slc27a1, Vdr). Molecular docking predicted strong binding affinities for several compound-target pairs, including Withanolide D-VDR (-12.0 kcal/mol) and 12-Deoxywithastramonolide-EPHX2 (-11.5 kcal/mol). Molecular dynamics simulations confirmed the structural stability of both top-ranked complexes over 100 ns, with low RMSD values and well-defined free energy minima. **Conclusions**: This in-silico study identified candidate targets and bioactive compounds that may be associated with the potential effects of the Xinbao Pill in HFpEF. The identified key targets and compounds may serve as promising candidates for further experimental validation and therapeutic development.

Keywords: Heart failure with preserved ejection fraction; Molecular docking; Network pharmacology; Traditional Chinese medicine; Xinbao Pill

Submitted on 30-05-2026 – Revised on 17-08-2026 – Accepted on 20-08-2026

Article in Press

INTRODUCTION

Heart failure with preserved ejection fraction (HFpEF) accounts for nearly half of heart failure cases worldwide and is a significant cause of morbidity and mortality (Borlaug, Sharma *et al*., 2023, Campbell, Rutten *et al*., 2024). Despite its growing prevalence, effective treatment options remain limited, although recent progress sodium-glucose cotransporter 2 (SGLT2) inhibitors and glucagon-like peptide-1 (GLP-1) receptor agonists has demonstrated encouraging cardiovascular benefits in HFpEF patients (Ni, Feng *et al*., 2024, Patel, Wadid *et al*., 2024). HFpEF is characterized by a multifactorial pathophysiology involving systemic inflammation, microvascular dysfunction, myocardial fibrosis and metabolic dysregulation (Hamo, DeJong *et al*., 2024). Heart failure with reduced ejection fraction has benefited from evidence-based therapies that have improved outcomes; however, HFpEF remains a treatment challenge, highlighting the urgent need for innovative approaches to identify new therapeutic targets and develop effective treatment strategies for this condition, which is on the rise.

Traditional Chinese medicine (TCM) has a long history of application in cardiovascular healthcare and Xinbao Pill has been investigated as an adjunctive therapy for chronic heart failure in both clinical and experimental settings (Huang, Li *et al*., 2022, Tian, Huang *et al*., 2023, Wang, Li *et al*., 2022). Xinbao Pill is a classic TCM formulation composed of four herbal medicines: *Panax notoginseng* (Sanqi), *Datura metel* (Yangjinhua), *Panax ginseng* (Renshen) and *Borneolum syntheticum* (Bingpian). Previous investigations have shown sustained clinical interest in Xinbao Pill and suggested potential benefits for cardiac function and adverse remodeling in heart failure (Chen, Luo *et al*., 2025, Wang, Li *et al*., 2022).

Understanding the molecular mechanisms underlying these effects is challenging because TCM preparations often contain multiple active compounds that act on distinct molecular targets. Network pharmacology has become an important method for studying the mechanisms of TCM formulas (Gao, Cao *et al*., 2021, Li and Zhang, 2013). A recent experimental study demonstrated that Xinbao Pill ameliorates chronic heart failure by regulating the SGLT1/AMPK/PPARα axis to improve myocardial fatty acid energy metabolism (Pan, Xu *et al*., 2024). This study provided valuable mechanistic evidence for a validated

**Corresponding author:* e-mail: wuyemenghan@163.com

pathway in chronic heart failure; however, it did not specifically address HFpEF. The present study used an integrated network pharmacology approach to generate a broader set of HFpEF-specific candidate targets and compound-target interactions by combining transcriptomic analysis, machine learning-based target identification and molecular docking validation. This integrated in silico approach provides a structured set of computational hypotheses that can guide subsequent experimental validation.

MATERIALS AND METHODS

Screening of active compounds from Xinbao Pill

The components of Xinbao Pill were obtained from the Traditional Chinese Medicine Systems Pharmacology Database and Analysis Platform (TCMSP) (Ru, Li *et al*., 2014). The following pharmacokinetic criteria were applied for initial screening, modified from Lipinski's Rule of Five: molecular weight (MW) ≤500, octanol/water partition coefficient (AlogP) ≤5, number of hydrogen bond donors (Hdon) ≤5, number of hydrogen bond acceptors (Hacc) ≤ 10, oral bioavailability (OB) ≥30% and drug-likeness (DL) ≥0.18. These thresholds are the standard filters implemented in TCMSP and are widely used in network pharmacology studies of traditional Chinese medicine to enrich orally available drug-like compounds (Li and Zhang, 2013).

Compounds that met these criteria were subsequently analyzed with the SwissADME web server (http://www.swissadme.ch) to assess additional pharmacokinetic properties (Daina, Michielin *et al*., 2017). Only compounds with acceptable drug-like properties and high gastrointestinal absorption were retained. The Swiss Target Prediction database (http://www.swisstargetprediction.ch) was used to predict potential targets for the selected compounds, with the species restricted to *Mus musculus* (Daina, Michielin *et al*., 2019). The top 100 predicted targets per compound were retained without applying an additional probability cutoff to maximize sensitivity for downstream intersection with HFpEF-related differentially expressed genes (DEGs). OB values are model-derived scores from TCMSP; values exceeding 100% do not represent true fractional absorption but rather result from the prediction algorithms.

Transcriptomic data acquisition and differential expression analysis

Three RNA-seq datasets related to HFpEF were obtained from the Gene Expression Omnibus (GEO) database, all derived from *Mus musculus* models to maintain species consistency with target prediction: GSE180065 (control n=5, HFpEF n=10; Illumina NovaSeq 6000), GSE240400 (control n=5, HFpEF n=5; C57Bl6 mice fed a standard diet or high-fat diet plus L-NAME for 6 weeks; Illumina NovaSeq 6000) (Mesquita, Miguel-Dos-Santos *et al*.) and GSE269053 (control n=4, HFpEF n=6; male C57BL/6NJ mice fed a 60% kcal high-fat diet for 10 weeks and randomized to receive AAV8-driven Renin1d overexpression or null vector; Illumina NovaSeq 6000) (Berger, Shi *et al*.). Differential expression analysis was performed separately for each dataset using the DESeq2 package in R (Love, Huber *et al*., 2014), with thresholds set at $|\log2FC| > 0.585$ (fold change > 1.5) and adjusted $P < 0.05$. Because the datasets were generated by independent studies with different experimental designs, cross-dataset batch correction was not the primary strategy.

Functional enrichment analysis and network construction

Gene Ontology (GO) enrichment analysis (Ashburner, Ball *et al*., 2000) and Kyoto Encyclopedia of Genes and Genomes (KEGG) pathway analysis (Kanehisa, 2000) were performed for both HFpEF-related DEGs and Xinbao Pill target genes using the clusterProfiler package in R (Yu, Wang *et al*., 2012). Statistical significance was assigned to terms with an adjusted p-value < 0.05.

The overlapping genes between HFpEF-related DEGs and Xinbao Pill target genes were identified using Venn diagram analysis. These intersecting genes and their active compounds were used to construct a compound-target network using Cytoscape software (Shannon, Markiel *et al*., 2003).

Machine learning-based key gene selection

Elastic Net regression was employed to refine the intersecting genes further and identify key targets associated with HFpEF (Friedman, Hastie *et al*., 2010, Vinga, 2020). The Elastic Net model combines L1 and L2 regularization, with alpha set to 0.7 to balance between LASSO (alpha=1) and Ridge regression (alpha=0). This alpha value was chosen to prioritize sparse feature selection while maintaining some degree of regularization stability. The $\lambda.1se$ value was selected by 10-fold cross-validation as the most regularized model with a cross-validation error within 1 standard error of the minimum. Genes with nonzero coefficients in the final model were selected as key genes. To assess the stability of the alpha choice, a sensitivity analysis was performed across alpha values from 0 to 1 in increments of 0.1; alpha = 0.7 yielded a near-minimum cross-validation deviance and selected 11 genes, supporting its use as a parsimonious yet predictive model.

Molecular docking analysis

The RCSB Protein Data Bank (PDB) provided the three-dimensional structures of candidate target proteins (Berman, 2000). The PDB IDs used were 6G33 (CLK1), 3A7E (COMT), 9BS9 (DRD2), 8QVF (EPHX2), 7UY0 (FGR), 3U10 (HCN2), 2YB9 (MME), 2Q59 (PPARG), 2WWP (PTGDS) and 1IE8 (VDR). Protein structures were prepared by removing water molecules and adding

Article in Press

hydrogen atoms. For each protein, the grid box center and size were defined according to the co-crystallized ligand-binding site, with typical dimensions of 20-25 Å in each direction.

Before production of the docking, redocking validation was performed using native co-crystal ligands to verify the docking protocol. All proteins showed acceptable redocking results with root mean square deviation (RMSD) values ≤ 2.5 A, confirming the reliability of the docking parameters. Molecular docking was performed using AutoDock Vina between each key protein and the 32 selected active compounds (Trott and Olson, 2009). The best predicted binding affinity for each protein-ligand pair was recorded and the best-ranked complexes were visualized using PyMOL. The binding modes were analyzed for hydrogen bonding and hydrophobic interactions with essential amino acid residues at the functional binding sites.

Molecular dynamics simulations

All-atom MD simulations were performed using GROMACS 2025.3 (Páll, Zhmurov *et al*.). Proteins were parameterized with the AMBER14SB force field (Maier, Martinez *et al*.). Ligand topologies and partial charges were generated using the general AMBER force field with AM1-BCC charges (Wang, Wolf Rm Fau - Caldwell *et al*.). Complexes were solvated in cubic TIP3P water boxes with 150 mM NaCl (Lu and Chen, 2021). Systems were energy-minimized using 500 steps of conjugate-gradient minimization, followed by 100 ps of position-restrained MD and 100 ns of production MD (2 fs time step). Temperature was maintained at 298.15 K using a V-rescale thermostat (τ = 0.2 ps) and pressure at 1.0 bar using a C-rescale barostat (τ = 0.5/2.0 ps). Hydrogen bonds were constrained with LINCS; long-range electrostatics were treated with PME (1.0 nm cutoff) and van der Waals interactions with a Verlet cutoff (1.0 nm) with dispersion corrections.

Trajectory analysis included RMSD of Cα atoms and ligand heavy atoms, radius of gyration (Rg), per-residue root mean square fluctuation (RMSF), SASA and protein-ligand hydrogen bonding. Free energy landscapes were constructed as functions of RMSD and Rg.

RESULTS

Screening of active compounds of Xinbao Pill

To identify candidate active compounds with favorable druggability, the chemical constituents of Xinbao Pill were first screened using the TCMSP database according to the following criteria: MW ≤ 500, AlogP ≤ 5, Hdon ≤ 5, Hacc ≤ 10, OB ≥30% and DL ≥ 0.18. Subsequently, the pharmacokinetic properties were evaluated using the SwissADME database and only compounds with acceptable drug-likeness and high gastrointestinal absorption were retained. Ultimately, 32 active compounds were identified after removal of duplicates (Table 1).

Identification and functional enrichment analysis of HFpEF-related DEGs

Differential expression analysis across the three GEO datasets revealed marked but variable transcriptomic alterations in HFpEF (Figs. 1A-1C). GO and KEGG enrichment analysis of the union of DEGs identified three major functional categories. KEGG pathway analysis showed prominent enrichment in cytokine-cytokine receptor interaction (33 genes), PPAR signaling pathway (15 genes) and cholesterol metabolism (10 genes). Among the top enriched terms at the molecular function level were metal ion transmembrane transporter activity (47 genes), immune receptor activity (23 genes) and cytokine receptor activity (19 genes). Together, these findings suggest that the HFpEF transcriptome is marked by inflammatory signaling, metabolic disruptions and changes in ion transport (Fig. 1D).

Enrichment analysis of Xinbao Pill target genes identified biological processes related to the regulation of blood circulation (47 genes) and vascular processes in the circulatory system (45 genes). According to KEGG pathway analysis, the most enriched pathways were neuroactive ligand receptor interaction (69 genes), calcium signaling pathway (45 genes) and neuroactive ligand signaling (38 genes). Protein serine/threonine kinase activity (46 genes), protein serine kinase activity (42 genes) and protein tyrosine kinase activity (36 genes) were the most significant terms at the molecular function level (Fig. 1E).

Comparison of the two enrichment profiles indicated a partial overlap in their functions. The DEGs associated with HFpEF were largely connected to inflammatory and metabolic pathways, whereas the targets of Xinbao Pill were enriched in circulatory regulation, calcium signaling and kinase activity. These functional overlaps support the subsequent identification of shared disease-drug targets.

Identification of intersecting targets and screening of key genes

Intersection analysis between the combined HFpEF-related DEGs and Xinbao Pill target genes yielded 23 overlapping genes (Fig. 2A). The compound-target network constructed from these intersecting genes and their corresponding active compounds contained 54 nodes connected by 199 edges, with an average degree of 7.37. The top hub compounds by degree were celabenzine (degree = 10), withanolide derivative 1 (degree = 9) and 12-Deoxywithastramonolide (degree = 9). The top hub proteins were Pde7a (degree = 19), Clk1 (degree = 19) and Adora2b (degree = 18) (Fig. 2B).

Article in Press

Table 1: Active compounds identified from Xinbao Pill with favorable pharmacokinetic properties.

Herb/MolID	Molecule Name	DL	OB	MW	AlogP	Hdon	Hacc	CAS
Bingpian								
MOL006861	asiatic acid	0.71	41.38	488.78	4.3	4	5	464-92-6
MOL006862	bronyl acetate	0.51	59.3	447.55	4.02	1	8	20347-65-3
Renshen								
MOL000422	kaempferol	0.24	41.88	286.25	1.77	4	6	136945-65-8
MOL000787	Fumarine	0.83	59.26	353.4	2.95	0	6	520-18-3
MOL003648	Inermin	0.54	65.83	284.28	2.44	1	5	50816-74-5
MOL005308	Aposiopolamine	0.22	66.65	271.34	1.39	1	4	52691-06-2
MOL005314	Celabenzine	0.49	101.88	379.55	2.29	2	5	130-86-9
MOL005318	Dianthramine	0.2	40.45	289.26	2.05	5	7	23095-44-5
MOL005321	Frutinone A	0.34	65.9	264.24	2.7	0	4	19908-48-6
MOL005356	Girinimbin	0.31	61.22	263.36	4.6	1	1	38210-27-4
MOL005360	malkangunin	0.63	57.71	432.56	1.84	2	7	
MOL005384	suchilactone	0.56	57.52	368.41	3.73	0	6	53938-08-2
Sanqi								
MOL001792	Liquiritigenin	0.18	32.76	256.27	2.57	2	4	578-86-9
MOL000098	quercetin	0.28	46.43	302.25	1.5	5	7	73123-10-1
Yangjinhua								
MOL003644	Withaferine	0.73	33.14	470.66	3.25	2	6	5119-48-2
MOL005406	atropine	0.19	45.97	289.41	1.72	1	4	51-55-8
MOL011519	hyoscine	0.27	49.84	303.39	0.82	1	5	138-12-5
MOL011531	Secowithamerclin	0.89	50.21	468.69	4.3	1	5	
MOL011499	Daturameteline A	0.73	50.4	486.66	2	3	7	
MOL011497	Withanolide derivative 1	0.9	53.86	454.66	3.89	2	5	
MOL011490	Datumetelin	0.68	56.04	468.69	3.64	0	5	
MOL011540	withanolide D	0.76	58.29	454.66	4.34	1	5	30655-48-2
MOL011093	apohyoscine	0.25	59.68	285.37	1.93	0	4	535-26-2
MOL011487	Datuarmeteloside B	0.75	62.06	470.66	3.18	2	6	
MOL003283	Tetralin derivative	0.39	66.51	360.44	2.25	4	6	26568-14-9
MOL001554	Scopolamine	0.27	67.97	303.39	0.82	1	5	51-34-3
MOL011498	Withanolide derivative 2	0.68	81.26	468.69	3.64	0	5	
MOL011539	Withametelin	0.77	83.59	436.64	4.34	0	4	
MOL011491	Datum tine	0.18	84.74	275.38	2.3	0	4	67078-20-0
MOL007923	Phenylprop-2-enoate derivative	0.21	93.36	284.33	3.52	2	4	
MOL011470	12-Deoxywithastramonolide	0.75	109.97	472.68	3.2	2	6	60124-17-6
MOL000631	Coumaroyl tyramine	0.2	112.9	283.35	2.88	3	4	20375-37-5

MW, molecular weight; OB, oral bioavailability; DL, drug-likeness; AlogP, atom-based calculated logP; Hacc, hydrogen bond acceptors; Hdon, hydrogen bond donors; CAS, Chemical Abstracts Service registry number.

Elastic Net regression was applied to the 23 intersecting genes for further screening. The model selected 11 genes with non-zero coefficients under the 1 standard error criterion (lambda.1se) (Figs. 2C and 2D). The expression heatmap confirmed distinct patterns between the control and HFpEF groups for these 11 genes (Fig. 2E).

Molecular docking analysis

Molecular docking was performed between the 11 significant proteins and 32 selected active compounds. The docking heatmap showed marked differences in binding affinities among different protein-ligand pairs (Fig. 3A).

Among all docking results, Withanolide D-VDR exhibited the highest binding affinity, achieving a top binding energy of -12.0 kcal/mol. In addition, 12-Deoxywithastramonolide-EPHX2 also exhibited high affinity, with its best binding energy recorded at -11.5 kcal/mol (Figs. 3B and 3C). To further illustrate the binding modes of the top-ranked protein–ligand complexes, the remaining four key docking pairs were visualized in three dimensions. The results showed that Withanolide D-DRD2 had the best binding affinity of -11.4 kcal/mol, followed by Suchilactone-CLK1(-10.8 kcal/mol), Withanolide D-FGR (-10.7 kcal/mol) and 12-Deoxywithastramonolide-PPARG (-10.5 kcal/mol) (Figs. 4A-4D).

Inspection of the docking conformations showed that all ligands could fit into the corresponding binding pockets and form hydrogen bonds with key amino acid residues.

Article in Press

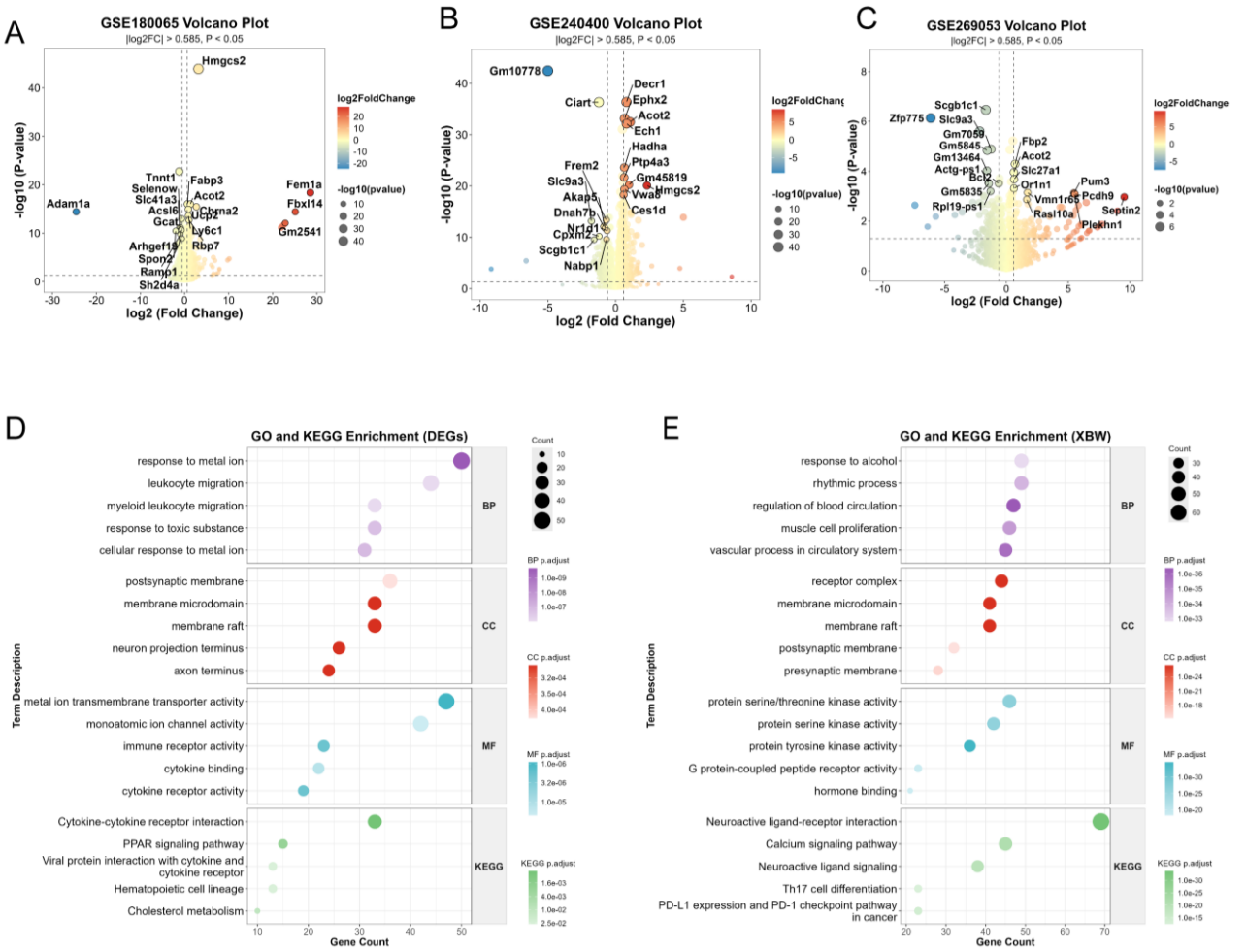


Fig. 1: Functional enrichment analyses of merged HFpEF-related differentially expressed genes and Xinbao Pill target genes. (A–C) Volcano plots of DEGs in three GEO datasets (GSE180065, GSE240400 and GSE269053). The x-axis represents log2 fold change and the y-axis represents -log10 p value. The dashed lines indicate the screening thresholds (|log2FC| > 0.585 and adjusted P < 0.05). Colors represent the magnitude of differential expression and dot sizes indicate statistical significance; (D) GO and KEGG enrichment analyses of the merged DEGs, including biological process (BP), cellular component (CC), molecular function (MF) and KEGG pathways; (E) GO and KEGG enrichment analyses of Xinbao Pill target genes, including BP, CC, MF and KEGG pathways. Bubble size indicates gene count and color denotes adjusted significance. Enrichment terms were selected and ranked using adjusted p-value and gene count.

Molecular dynamics simulation analysis

To assess the dynamic stability of the top docking complexes, 100 ns all-atom MD simulations simulations were performed for the Withanolide D-VDR and 12-Deoxywithastramonolide-EPHX2 complexes.

For the Withanolide D-VDR system, the ligand RMSD fluctuated mainly within a narrow range of approximately 0.8-1.2 A after initial equilibration, indicating that the ligand maintained a stable conformation within the complex throughout the simulation. The protein and complex trajectories fluctuated predominantly around 2.6-3.2 A during the middle of the simulation and reached approximately 3.0-3.5 A toward 100 ns (Fig. 5A), without abrupt or sustained structural divergence. The VDR RMSF was generally approximately 0.6-1.8 A; localized peaks were confined to flexible segments and did not indicate global structural destabilization (Fig. 5B). Consistent with the RMSD and RMSF profiles, the free energy landscape showed a dominant low-energy basin at an RMSD of approximately 2.5-3.5 Å, supporting the presence of a stable, preferentially populated conformational state (Fig. 5C).

For the 12-Deoxywithastramonolide-EPHX2 system, the protein and complex RMSD values increased during the initial conformational adjustment and, after approximately 40 ns, fluctuated within a narrow range of approximately 2.4-2.7 A. The ligand RMSD remained mainly around 0.7-1.2 A, with only occasional excursions to approximately 1.4 A (Fig. 5D), indicating that the ligand conformation remained stable within the complex.

Article

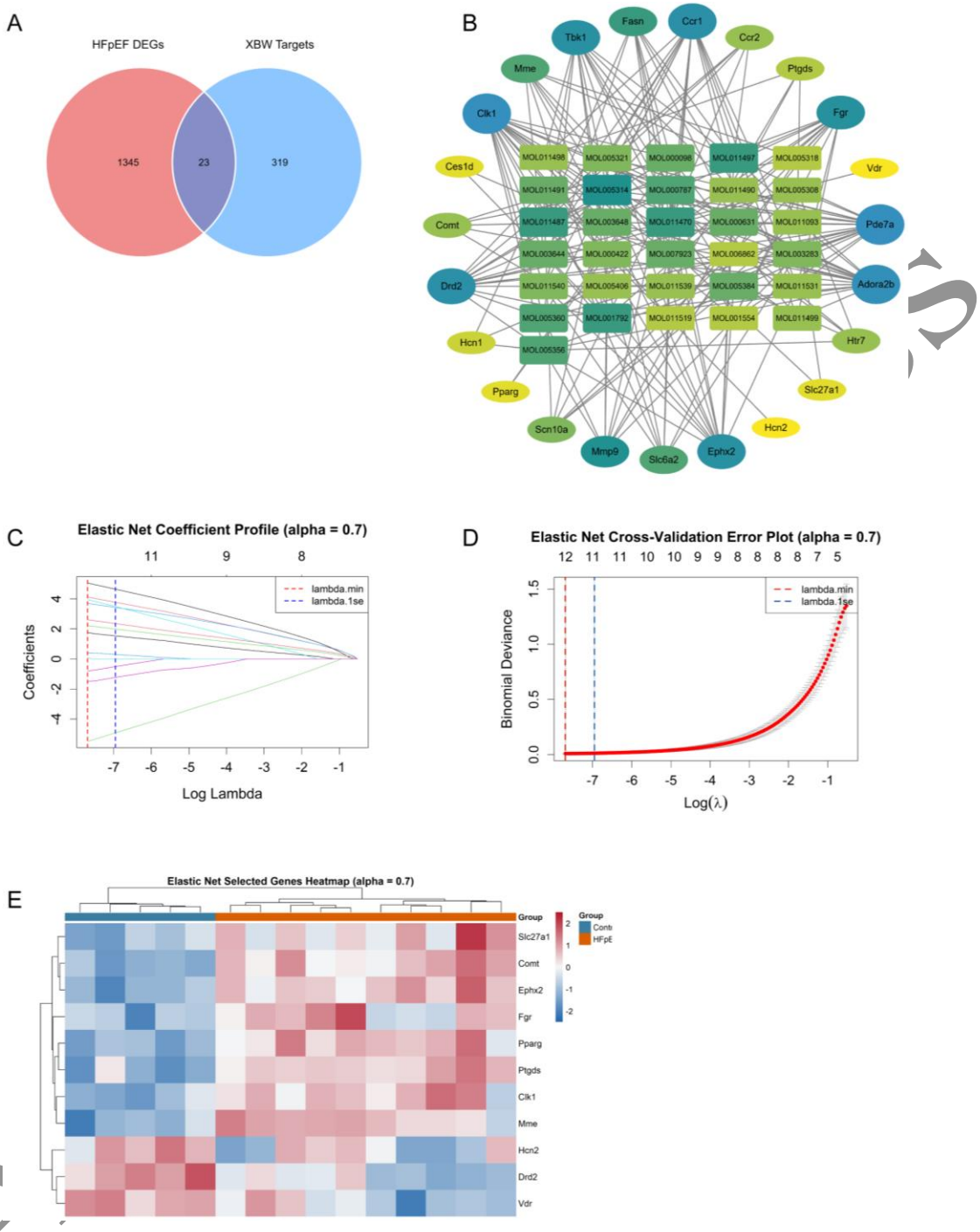


Fig. 2: Intersection analysis between merged HFpEF-related DEGs and Xinbao Pill target genes and identification of characteristic genes. (A) Venn diagram showing the overlap between merged HFpEF-related DEGs and Xinbao Pill target genes, yielding 23 intersecting genes; (B) Compound-target network of the intersecting genes and their corresponding active compounds. Square nodes represent active compounds of Xinbao Pill, oval nodes represent intersecting protein targets and edges indicate predicted compound-target associations. Node color is proportional to degree (number of connections); (C) Coefficient profile plot of the Elastic Net model (alpha = 0.7). As the penalty parameter lambda changes, the regression coefficients of different genes gradually shrink; (D) Cross-validation error plot of the Elastic Net model (alpha = 0.7). The vertical dashed lines indicate lambda.min (red) and lambda.1se (blue); the lambda.1se was used to select the most regularized model whose error was within one standard error of the minimum, retaining 11 genes; (E) Heatmap showing the expression patterns of the 11 Elastic Net-selected genes between the control and HFpEF groups. The color intensity represents the normalized gene expression levels.

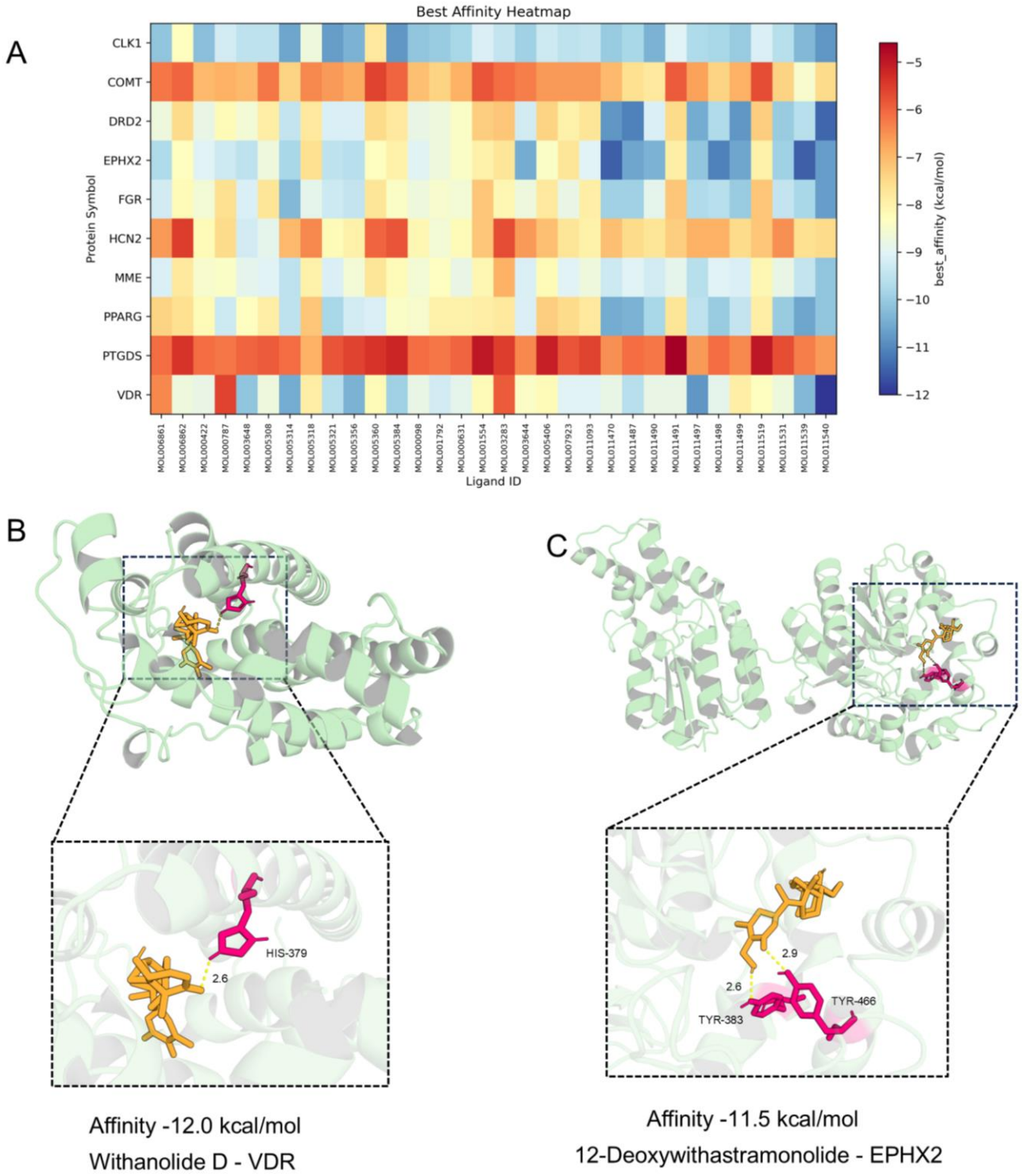


Fig. 3: Molecular docking analysis of key target proteins and active compounds. (A) Heatmap of the best docking affinities between 11 key proteins and 32 active compounds. the color scale indicates the best binding affinity (kcal/mol); (B) Molecular docking visualization of the Withanolide D-VDR complex, with a best binding affinity of -12.0 kcal/mol; (C) Molecular docking visualization of the 12-Deoxywithastramonolide-EPHX2 complex, with a best binding affinity of -11.5 kcal/mol. In the docking models, green indicates the protein structure, orange indicates the ligand molecule, yellow indicates hydrogen bonds and red indicates key amino acid residues.

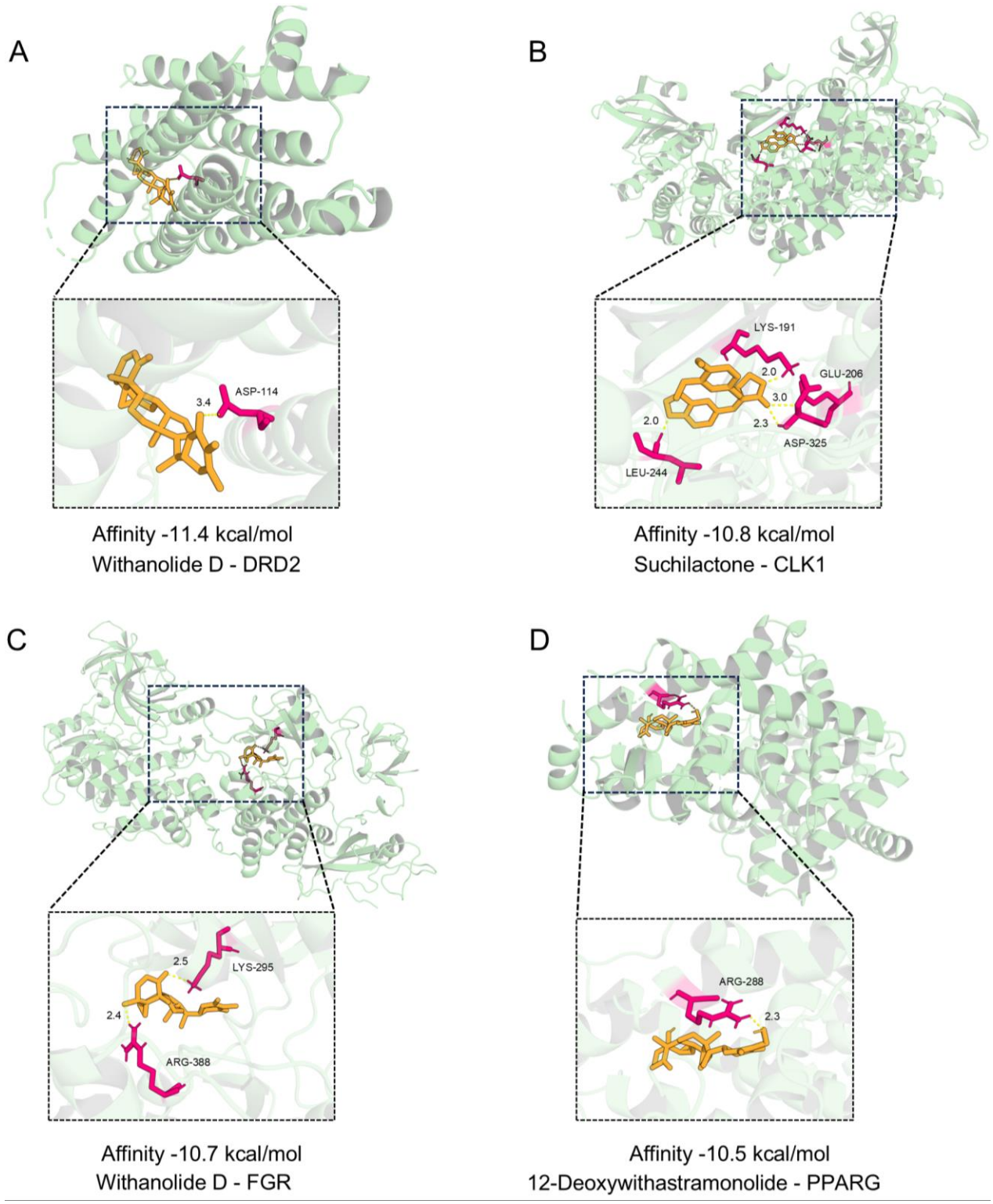


Fig. 4: Molecular docking visualizations of the remaining key protein–active compound complexes. (A) Molecular docking visualization of the Withanolide D-DRD2 complex, with the best binding affinity of -11.4 kcal/mol; (B) Molecular docking visualization of the Suchilactone-CLK1 complex, with the best binding affinity of -10.8 kcal/mol; (C) Molecular docking visualization of the Withanolide D-FGR complex, with the best binding affinity of -10.7 kcal/mol; (D) Molecular docking visualization of the 12-Deoxywithastramonolide-PPARG complex, with the best binding affinity of -10.5 kcal/mol. In the docking models, green indicates the protein structure, orange indicates the ligand molecule, yellow indicates hydrogen bonds and red indicates key amino acid residues.

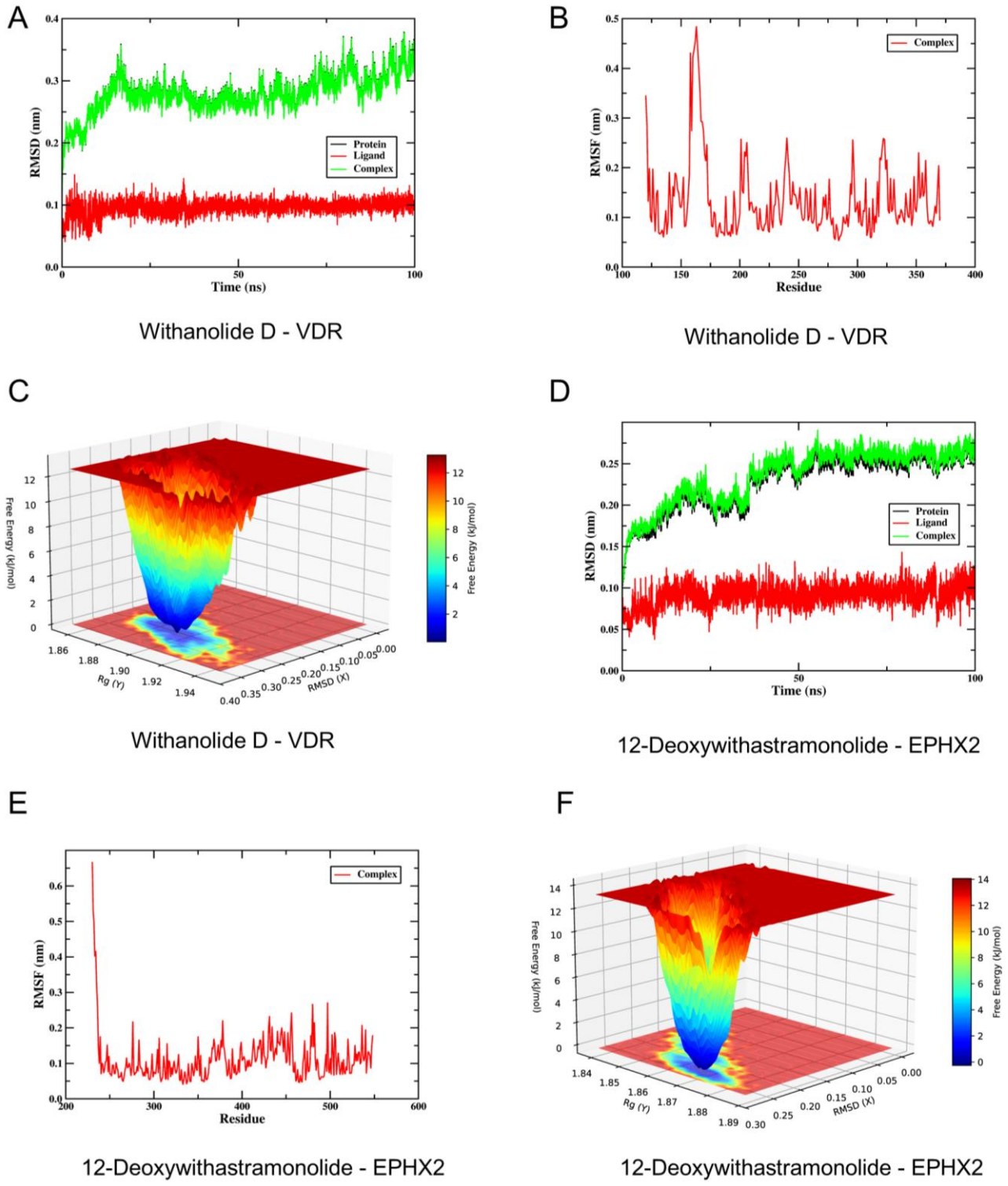


Fig. 5: Molecular dynamics simulation analysis of the top two protein-ligand complexes. (A) RMSD plot of the Withanolide D-VDR complex over 100 ns, showing protein backbone (black), ligand (red) and complex (green) RMSD values; (B) Per-residue RMSF of the VDR protein in complex with Withanolide D; (C) Free energy landscape of the Withanolide D-VDR complex as a function of RMSD and radius of gyration; (D) RMSD plot of the 12-Deoxywithastramonolide-EPHX2 complex over 100 ns; (E) Per-residue RMSF of the EPHX2 protein in complex with 12-Deoxywithastramonolide; (F) Free energy landscape of the 12-Deoxywithastramonolide-EPHX2 complex (1 nm = 10 A).

Across residues 250-550, the EPHX2 RMSF was predominantly approximately 0.6-1.5 A; localized peaks of approximately 2.0-2.7 A and the pronounced N-terminal peak reflected regional flexibility rather than global structural instability (Fig. 5E). The free energy landscape showed a concentrated low-energy basin at an RMSD of approximately 2.0-2.7 A, further indicating that the complex preferentially occupied a stable conformational state (Fig. 5F).

Collectively, the narrow post-equilibration RMSD fluctuations, generally low residue-level RMSF values and concentrated low-energy basins demonstrate that both protein–ligand complexes remained structurally and conformationally stable during the 100 ns simulations. These results provide dynamic evidence supporting the stability of the docking-derived Withanolide D-VDR and 12-Deoxywithastramonolide-EPHX2 binding models.

DISCUSSION

This study used a network pharmacology approach to systematically investigate the potential molecular mechanisms underlying the effects of Xinbao Pill in HFpEF. Through multistage analyses, 32 active compounds from Xinbao Pill and 11 key HFpEF-related targets were identified and favorable binding affinities were predicted for several compound-target pairs. This systems-level framework is consistent with recent methodological reviews highlighting the utility of network pharmacology for dissecting multi-component TCM interventions in heart failure and other complex cardiovascular disorders (Gao, Cao *et al*., 2021).

The identified targets are associated with several biological processes relevant to HFpEF. HFpEF is commonly accompanied by metabolic stress, low-grade inflammation, endothelial and microvascular dysfunction, myocardial fibrosis and impaired relaxation. In this context, VDR, EPHX2, FGR and CLK1 may be particularly involved in inflammatory and fibrotic remodeling. VDR signaling is associated with cardiac remodeling and immune regulation (Gardner, Chen *et al*., 2013), whereas EPHX2 regulates epoxyeicosatrienoic acid metabolism and may affect vascular inflammation and cardioprotective lipid signaling (Jiang, Han *et al*., 2024). FGR and CLK1 may further connect the candidate network with stress-responsive signaling and cellular remodeling pathways. These targets suggest a possible route through which Xinbao Pill may influence the inflammatory and fibrotic components of HFpEF, both of which contribute to myocardial stiffness and diastolic dysfunction.

The candidate target profile also suggests an association with metabolic disturbances. PPARG is a major regulator of lipid metabolism and insulin sensitivity and SLC27A1 is involved in fatty acid transport (Montaigne, Butruille *et al*., 2021, Quiriarte, Noland *et al*., 2024). These findings are relevant because obesity, insulin resistance, altered fatty acid handling and mitochondrial stress are common features of HFpEF (Hamo, DeJong *et al*., 2024). These findings align with a recent study by Pan *et al*., which demonstrated that Xinbao Pill regulates the SGLT1/AMPK/PPARα axis in chronic heart failure (Pan, Xu *et al*., 2024). This study provides mechanistic evidence for the regulation of energy metabolism in patients with chronic heart failure.

The network topology identified additional mediators that were not retained in the final Elastic Net model. PDE7A and CLK1 showed the highest degrees in the compound-target network and ADORA2B ranked highly. PDE7A regulates intracellular cAMP signaling, which influences cardiac contractility and inflammation (Calamera, Moltzau *et al*., 2022). CLK1 regulates transcript splicing through the phosphorylating serine/arginine-rich splicing factors, suggesting a potential link between Xinbao Pill-associated targets and stress-responsive remodeling programs (Song, Pang *et al*., 2023). ADORA2B is an adenosine receptor associated with tissue fibrosis and cardioprotective responses (Effendi and Nagano, 2023). These highly connected targets suggest that compounds in Xinbao Pill exert broad regulatory effects, potentially underlying its polypharmacological actions.

Several active compounds identified in the Xinbao Pill have demonstrated cardiovascular benefits in previous studies. Withanolide-type steroidal lactones, particularly withaferin A-related compounds, exhibit anti-inflammatory activity and have attracted growing interest in cardiovascular applications (Logie and Vanden Berghe, 2020, Wiciński, Fajkiel-Madajczyk *et al*., 2024). These compounds have been reported to modulate signaling pathways involved in cardiac remodeling, notably TGF-beta and NF-kappaB mediated responses. Furthermore, quercetin, another recurrent compound identified in the network, exhibits broad cardioprotective, antioxidant and anti-inflammatory activities that may be relevant to HFpEF pathobiology (Ferenczyova, Kalocayova *et al*., 2020). Therefore, the predicted binding affinities are structurally plausible, but they remain computational estimates and absolute scores cannot be equated with *in-vivo* potency or clinical efficacy. To further support these docking predictions, molecular dynamics simulations of the two top-ranked complexes, Withanolide D-VDR and 12-Deoxywithastramonolide-EPHX2, showed stable binding throughout the simulations, with low RMSD values, preserved binding-site rigidity and well-defined free energy minima, suggesting that the top-ranked docking poses represent energetically stable binding modes rather than transient conformations.

Network analysis revealed a complex interaction pattern between Xinbao Pill compounds and HFpEF-related

Article in Press

targets, with multiple compounds targeting multiple genes and vice versa. Topological analysis of the network revealed primary hub compounds, including celabenzine, withanolide derivative 1, datuarmeteloside B, 12-deoxywithastramonolide and liquiritigenin, with each compound connected to 9-10 target proteins. Multiple compounds targeted hub proteins, such as Pde7a, Clk1 and Adora2b, indicating their potential role as key mediators in the therapeutic effects of Xinbao Pill. This network pattern suggests that Xinbao Pill may act through multiple compounds and targets, which is consistent with the characteristics of traditional Chinese medicine. Enrichment analysis indicated that these predicted targets are implicated in key HFpEF-related biological processes and molecular functions, including circulatory regulation, kinase activity and neurohumoral signaling.

This study has several important limitations. First, all analyses are computational and require experimental verification. The three GEO datasets were small and were generated from different mouse HFpEF models; the union strategy was chosen to maximize sensitivity to heterogeneous disease signals, but it also increased the risk of model-specific false positives. Moreover, all GEO datasets originated from mouse models, which could limit their translation to human HFpEF. Molecular docking employed a rigid-receptor approximation; although complemented by molecular dynamics simulations for the two top-ranked complexes, these simulations are limited in scope and timescale and do not substitute for experimental binding validation.

To address these limitations, future investigations should integrate *in-vitro* and *in-vivo* validation. Specifically, the predicted binding affinities warrant experimental confirmation through *in-vitro* assays, followed by functional evaluation in cellular and animal models. Ultimately, a clinical trial of Xinbao Pill in patients with HFpEF, incorporating biomarker profiling of the identified hub targets, is warranted to validate these computational predictions.

The findings of this study have several potential clinical implications for further investigation. For patient stratification, the 11 key genes were developed into a gene expression signature to identify HFpEF patients who would benefit the most from Xinbao Pill therapy. In therapeutic development, the primary active compounds, particularly Withanolide D and 12-Deoxywithastramonolide, can serve as lead compounds for structural optimization to improve their efficacy, selectivity and pharmacokinetic properties. Additionally, the network pharmacology strategy adopted in this study might be used to examine other TCM formulas for cardiovascular diseases, potentially bridging traditional Chinese medicine with modern pharmacology.

CONCLUSION

In summary, this network pharmacology analysis identified 32 active compounds and 11 key target genes, systematically elucidating the molecular mechanisms underlying the therapeutic effects of Xinbao Pill in HFpEF. Molecular docking predicted favorable binding interactions and molecular dynamics simulations confirmed the structural stability of the top two complexes. Because all analyses were computational, these findings should be interpreted as hypotheses rather than established mechanisms. Further *in-vitro* and *in-vivo* experiments are needed to validate the biological relevance of the proposed compound-target interactions before any clinical or therapeutic conclusions can be drawn.

Acknowledgment of generative AI in scientific writing

During the preparation of this work, the authors used ChatGPT to assist with language editing and to improve manuscript readability. The authors have carefully reviewed and verified all the content and take full responsibility for the accuracy of the manuscript.

Author's contributions

JS: Conceptualization, investigation, writing - original draft; XY: Methodology and visualization. XZ: Investigation and writing-review and editing; SC: Methodology and writing-review and editing; DH: Conceptualization, methodology, visualization and writing-review and editing. All authors have read and approved the final version and agree to its submission.

Funding

This study was supported by the Science and Technology Plan Project of Taizhou (21ywb128), the Wenzhou Traditional Chinese Medicine Research Project Funding (Z2024003) and the Medical Science and Technology Project of Zhejiang Province (2023KY1350).

Data availability statement

The RNA-seq datasets analyzed during the current study are available in the NCBI GEO repository under accession numbers GSE180065, GSE240400 and GSE269053. The data generated or analyzed during this study will be available from the corresponding author upon request.

Ethical approval

Not applicable.

Conflict of interest

The authors declare no conflict of interest.

REFERENCES

Ashburner M, Ball CA, Blake JA, Botstein D, Butler H, Cherry JM, Davis AP, Dolinski K, Dwight SS, Eppig JT, Harris MA, Hill DP, Issel-Tarver L, Kasarskis A, Lewis

Article in Press

S, Matese JC, Richardson JE, Ringwald M, Rubin GM and Sherlock G (2000). Gene Ontology: Tool for the unification of biology. *Nat. Genet.*, **25**(1): 25-29.

Berger JH, Shi Y, Matsuura TR, Batmanov K, Chen X, Tam K, Marshall M, Kue R, Patel J, Taing R, Callaway R, Griffin J, Kovacs A, Hirenallur-Shanthappa D, Miller R, Zhang BB, Flach RJR and Kelly DP (2025). Two-hit mouse model of heart failure with preserved ejection fraction combining diet-induced obesity and renin-mediated hypertension. *Sci. Rep.*, **15**(1): 422.

Berman HM (2000). The Protein Data Bank. *Nucleic Acids Res.*, **28**(1): 235-242.

Borlaug BA, Sharma K, Shah SJ and Ho JE (2023). Heart Failure With Preserved Ejection Fraction. *J. Am. Coll. Cardiol.*, **81**(18): 1810-1834.

Calamera G, Moltzau LR, Levy FO and Andressen KW (2022). Phosphodiesterases and compartmentation of cAMP and cGMP signaling in regulation of cardiac contractility in normal and failing hearts. *Int. J. Mol. Sci.* **23**(4): 2145.

Campbell P, Rutten FH, Lee MMY, Hawkins NM and Petrie MC (2024). Heart failure with preserved ejection fraction: Everything the clinician needs to know. *Lancet.* **403**(10431): 1083-1092.

Chen W, Luo X, Li W, Li X, Wang Y, Zhang R, Liu B, Zhu L, Liu Z and Cheng Y (2025). Uncovering the active ingredients of Xinbao pill against chronic heart failure: A chemical profiling, pharmacokinetics and pharmacodynamics integrated study. *J. Ethnopharmacol.* **342**: 119418.

Daina A, Michielin O and Zoete V (2017). SwissADME: A free web tool to evaluate pharmacokinetics, drug-likeness and medicinal chemistry friendliness of small molecules. *Sci. Rep.*, **7** (1): 42717.

Daina A, Michielin O and Zoete V (2019). Swiss Target Prediction: Updated data and new features for efficient prediction of protein targets of small molecules. *Nucleic Acids Res.*, **47**(W1): W357-W364.

Effendi WI and Nagano T (2023). A2B adenosine receptor in idiopathic pulmonary fibrosis: Pursuing proper pit stop to interfere with disease progression. *Int. J. Mol. Sci.*, **24**(5): 4428.

Ferenczyova K, Kalocayova B and Bartekova M (2020). Potential implications of quercetin and its derivatives in cardioprotection. *Int. J. Mol. Sci.* ,**21**(5): 1585.

Friedman J, Hastie T and Tibshirani R (2010). Regularization paths for generalized linear models via coordinate descent. *J. Stat. Softw.*, **33**(1): 1-22.

Gao L, Cao M, Li Jq, Qin X-m and Fang J (2021). Traditional Chinese medicine network pharmacology in cardiovascular precision medicine. *Curr. Pharm. Des.*, **27**(26): 2925-2933.

Gardner DG, Chen S and Glenn DJ (2013). Vitamin D and the heart. *Am. J. Physiol. Regul. Integr. Comp. Physiol.*, **305**(9): R969-R977.

Hamo CE, DeJong C, Hartshorne-Evans N, Lund LH, Shah SJ, Solomon S and Lam CSP (2024). Heart failure with preserved ejection fraction. *Nat. Rev. Dis. Prim.*, **10**(1): 55.

Huang M, Li Z, Fan Y, Li D, Liu Q, Chen B, Peng Z and Ding B (2022). Clinical evidence of Xinbao Pills efficacy on chronic heart failure patients: A protocol for systematic review and meta-analysis. *Medicine.* **101**(39): e30764.

Jiang S, Han S and Wang DW (2024). The involvement of soluble epoxide hydrolase in the development of cardiovascular diseases through epoxyeicosatrienoic acids. *Front. Pharmacol.*, **15**: 1358256.

Kanehisa M (2000). KEGG: Kyoto encyclopedia of genes and genomes. *Nucleic Acids Res.*, **28**(1): 27-30.

Li S and Zhang B (2013). Traditional Chinese medicine network pharmacology: Theory, methodology and application. *Chin. J. Nat. Med.*, **11**(2): 110-120.

Logie E and Vanden Berghe W (2020). Tackling chronic inflammation with withanolide phytochemicals—A withaferin a perspective. *Antioxidants*, **9**(11): 1107.

Love MI, Huber W and Anders S (2014). Moderated estimation of fold change and dispersion for RNA-seq data with DESeq2. *Genome Biol.*, **15**(12): 550.

Lu T and Chen Q (2021). Shermo: A general code for calculating molecular thermochemistry properties. *Comput. Theor. Chem*., **1200**: 113249.

Maier JA, Martinez C, Kasavajhala K, Wickstrom L, Hauser KE and Simmerling C (2015) ff14SB: Improving the accuracy of protein side chain and backbone parameters from ff99SB. *J. Chem. Theory Comput.*, **11** (8): 3696-3713.

Mesquita T, Miguel-dos-Santos R, Liu W, Fournier M, Rogers RG, Alfaro J, Nawaz A, Sanchez L, Jones XM, Li L, Marbán E and Cingolani E (2025). Upregulated FoxO1 promotes arrhythmogenesis in mice with heart failure and preserved ejection fraction. . *Nat. Commun.*, **16**(1): 1184.

Montaigne D, Butruille L and Staels B (2021). PPAR control of metabolism and cardiovascular functions. *Nat. Rev. Cardiol.*,**18**(12) 809-823.

Ni XY, Feng XJ, Wang ZH, Zhang Y, Little PJ, Cao Y, Xu SW, Tang LQ and Weng JP (2024). Empagliflozin and liraglutide ameliorate HFpEF in mice via augmenting the Erbb4 signaling pathway. *Acta Pharmacol. Sin.*, **45**(8): 1604-1617.

Páll S, Zhmurov A, Bauer P, Abraham MJ, Lundborg M, Gray A, Hess B and Lindahl E (2020). Heterogeneous parallelization and acceleration of molecular dynamics simulations in GROMACS. *J. Chem. Phys.*, **153**(13): 134110.

Pan L, Xu Z, Wen M, Li M, Lyu D, Xiao H, Li Z, Xiao J, Cheng Y and Huang H (2024). Xinbao Pill ameliorates heart failure via regulating the SGLT1/AMPK/PPARα axis to improve myocardial fatty acid energy metabolism. *Chin. Med.*, **19**(1): 82.

Patel R, Wadid M, Makwana B, Kumar A, Khadke S, Bhatti A, Banker A, Husami Z, Labib S, Venesy D, Fonarow G, Kosiborod M, Al-Kindi S, Bhatt DL, Dani

Article in Press

S, Nohria A, Butler J and Ganatra S (2024). GLP-1 receptor agonists among patients with overweight or obesity, diabetes and HFpEF on SGLT2 inhibitors. *JACC Heart Fail.,* **12**(11): 1814-1826.

Quiriarte H, Noland RC, Stampley JE, Davis G, Li Z, Cho E, Kim Y, Doiron J, Spielmann G, Ghosh S, Shah SJ, Irving BA, Lefer DJ and Allerton TD (2024). Exercise therapy rescues skeletal muscle dysfunction and exercise intolerance in cardiometabolic HFpEF. *JACC Basic Transl. Sci.*, **9**(12): 1409-1425.

Ru J, Li P, Wang J, Zhou W, Li B, Huang C, Li P, Guo Z, Tao W, Yang Y, Xu X, Li Y, Wang Y and Yang L (2014). TCMSP: A database of systems pharmacology for drug discovery from herbal medicines. *J. Cheminform.,* **6**(1): 13.

Shannon P, Markiel A, Ozier O, Baliga NS, Wang JT, Ramage D, Amin N, Schwikowski B and Ideker T (2003). Cytoscape: A software environment for integrated models of biomolecular interaction networks. *Genome Res.,* **13**(11): 2498-2504.

Song M, Pang L, Zhang M, Qu Y, Laster KV and Dong Z (2023). Cdc2-like kinases: Structure, biological function and therapeutic targets for diseases. *Signal Transduct. Target. Ther.,* **8** (1): 148.

Tian X, Huang Z, Wang Y, Qi X, Wang D, Liu Z and Cheng Y (2023). Xinbao Pill attenuated chronic heart failure by suppressing the ubiquitination of β-adrenergic receptors. *Phytomedicine* **115**: 154830.

Trott O and Olson AJ (2009). AutoDock Vina: Improving the speed and accuracy of docking with a new scoring function, efficient optimization and multithreading. *J. Comput. Chem.,* **31**(2): 455-461.

Vinga S (2020). Structured sparsity regularization for analyzing high-dimensional omics data. *Brief. Bioinform.,* **22**(1): 77-87.

Wang J, Wolf RM, Caldwell JW, Kollman PA and Case DA (2004). Development and testing of a general amber force field. *J. Comput. Chem.,* **25**(9): 1157-1174.

Wang Y, Li J, Yan J, Wang Y, Cheng Y, Liu Z and Wang D (2022). Efficacy of Xinbao pill on chronic heart failure: Study protocol of a multicenter, randomized, double-blind, placebo-controlled trial. *Front. Pharmacol.,* **13**: 1058799.

Wiciński M, Fajkiel-Madajczyk A, Kurant Z, Liss S, Szyperski P, Szambelan M, Gromadzki B, Rupniak I, Słupski M and Sadowska-Krawczenko I (2024). Ashwagandha's multifaceted effects on human health: Impact on vascular endothelium, inflammation, lipid metabolism and cardiovascular outcomes-A review. *Nutrients.* **16**(15): 2481.

Yu G, Wang LG, Han Y and He QY (2012). ClusterProfiler: An R package for comparing biological themes among gene clusters. *OMICS.* **16**(5): 284-287.

Article in Press